APPLIED ORGANOMETALLIC CHEMISTRY, VOL. 11, 601–616 (1997)

# Organometallic Complexes with Biological Molecules: VIII. Synthesis, Solid State and *in vivo* Investigation of Triorganotin(IV) Derivatives of L-Homocysteic Acid

Alessandro Pellerito,[1] Tiziana Fiore,[1] Anna Maria Giuliani,[1] Francesco Maggio,[1] Lorenzo Pellerito,[1]* Roberto Vitturi,[2] M. Stella Colomba[2] and Rainer Barbieri[3]
[1] Dipartimento di Chimica Inorganica, Università di Palermo, Via Archirafi 26, 90123 Palermo, Italy
[2] Istituto di Zoologia, Università di Palermo, Via Archirafi 18, 90123 Palermo, Italy
[3] Dipartimento di Biologia Cellulare e dello Sviluppo 'A. Monroy', Università di Palermo, Parco D'Orleans 2, 90128 Palermo, Italy

**Several new triorganotin(IV) derivatives of L-homocysteic acid (L-HCAH) with formula $R_3Sn$(L-HCA) (R = Me, $^n$Bu, Ph) have been synthesized. Their solid-state configurations were determined by IR and Mössbauer spectroscopy. The tin(IV) atom is five-coordinated in all the complexes, with the L-homocysteic acid behaving as a monoanionic bidentate ligand coordinating the tin(IV) atom through a chelating or bridging carboxylate group. The sulfonate ($SO_3^-$) and $NH_3^+$ groups of L-homocysteic acid maintain their free acid configuration and hence do not participate to the coordination of the tin(IV) atom. Coordination hypotheses have been checked through the correlation between the Mössbauer parameter isomer shift, $\delta$, and partial atomic charge on the tin atoms, $Q_{Sn}$, performed, for all the new organotin(IV) compounds, on the basis of an equalization procedure applied to idealized trigonal-bipyramidal structures for $R_3Sn$(L-HCA).**

**$^1$H and $^{13}$C NMR spectra of the complexes show that pentacoordination of the tin atom, with R groups in the equatorial plane of a trigonal bipyramid, is retained in DMSO solution. The NMR data confirm also that the uncoordinated $NH_3^+$ group of the ligand is still present in solution.**

**Results gathered after exposure of two- to four-cell embryos of the sea urchin *Paracentrotus lividus* (Echinodermata) to the triorganotin(IV) L-homocysteate derivatives as well as to the parent triorganotin(IV) chlorides document cytotoxicity of the complexes, while free L-homocysteic acid exerts no significant toxic activity. The trimethyltin(IV) L-homocysteate derivative seems to exert a lower cytotoxicity than the tributyl- and triphenyl-tin(IV) ones. Different structural lesions have been identified by comparative analysis of mitotic chromosomes from untreated embryos (negative controls) and embryos treated with triorganotin(IV) L-homocysteate derivatives, such as (1) suppression of the stretch among sister chromatids at the beginning of anaphase stage; (2) deeply stained zones mainly located at the telomeric regions of chromosomes; (3) arm breakages; and (4) chromosome bridges among daughter chromosomes at anaphase stage. A colchicine-like effect of triorganotin(IV) L-homocysteate derivatives was observed. © 1997 by John Wiley & Sons, Ltd.**

*Appl. Organometal. Chem.* **11**, 601–616 (1997)
No. of Figures: 20 No. of Tables: 6 No. of Refs: 45

**Keywords: Triorganotin(IV); L-homocysteic acid; Infrared; Mössbauer; NMR; Sea Urchin; *Paracentrotus lividus* (Echinodermata)**

*Received 31 May 1996; accepted 5 December 1996*

## INTRODUCTION

It has been clearly shown that the four subtypes of the excitatory amino-acid (EAA) receptors

* Correspondence to: Lorenzo Pellerito.
Contract grant sponsor: Ministero per l'Università e la Ricerca Scientifica e Tecnologica (MURST).

 CCC 0268–2605/97/070601–16 $17.50

[*N*-methyl-D-aspartate, NMDA; $\alpha$-amino-3-hydroxy-5-methyl isoxazole-4-propionate, AMPA; kainate, KA; and 2-amino-4-phosphonobutyrate, AP4] are very important in the synaptic excitation of the central nervous system in living organisms. This occurs by changing the effectiveness of the synapses involved in neuronal plasticity, memory acquisition and several further processes.[1] An excess of such excitatory amino acid receptors produces neurological disorders, mainly resulting in neurodegenerative processes. Consequently, this receptor family became the object of a number of research groups aiming to find agents able to modulate these receptor subtypes. In particular, the NMDA receptor has been widely investigated and much information has been accumulated, owing to its selective binding sites.[2] Among the NMDA agonists, one of the most powerful is L-homocysteic acid [L-2-amino-4-sulfobutyric acid], which is an endogenous constituent of the brain.[3] Its decrease may provoke hyperactivity of NMDA with consequential neurological disorders. In addition, many toxicological reports deal with encephalopathies and other neurological disorders following exposure to organotin(IV) derivatives, mainly represented by trimethyltin(IV) compounds.[4,5]

Adverse activity of these chemicals was found to be due to an interaction between organotin(IV) moieties and the EAA agonists. Following our work devoted to the study of the interactions between biological molecules present in living organisms and organotin(IV) moieties, we carried out the synthesis and structural solid-state characterization of the triorganotin(IV) L-homocysteate derivatives. Moreover, *in vivo* effects of free L-homocysteic acid, the triorganotin(IV) L-homocysteate derivatives and their triorganotin(IV) chloride parents, have been tested towards the mitotic chromosomes of the sea urchin *Paracentrotus lividus* (Echinodermata).

Previously, a number of semisynthetic antibiotics of organotin(IV) moieties had been prepared in our laboratory.[6–9] *In vivo* cytotoxic activity of these novel compounds was explored using several different tests. From these studies it was shown that cytotoxic implications occurred in biological systems such as cellular mitochondrial complexes and cytomembranes of the ascidian *Ciona intestinalis* embryos at early stages of development.[10]

Similarly, it was observed that adverse effects, mainly classifiable as formation of large decondensed regions, breakages and side-arm bridges, were present in mitotic chromosomes at the metaphase stage of *Aphanius fasciatus* (Pisces, Cyprinodontiformes)[7] and *Rutilus rubilio* (Pisces, Cypriniformes).[9]

It was also suggested that the anomalous development of *C. intestinalis* embryos following exposure to organotin(IV) complexes might be due to chromosomal disorders. Unfortunately, a useful analysis of *C. intestinalis* chromosomes was impossible due to the very small dimensions (1 to 2 $\mu$m) of the chromosomes of this species.[11]

In an attempt to overcome this difficulty we have chosen as a source of mitotic chromosomes for our experiments early developing embryos of the sea urchin *Paracentrotus lividus* (Echinodermata).

This species is particularly suitable for our purpose because:

(1) *P. lividus* embryos are supplied continuously as experimental material since they are routinely employed in molecular assays;[12] and
(2) mitotic chromosomes of this species[13] are considerably larger than those of *C. intestinalis*, thus allowing us to better evaluate possible chromosome abnormalities.

Three additional implications also support our choice. The first is that early developing embryos represent well a natural source of cleaving cells which, as a short-term culture, can provide abundant mitotic chromosome spreads. The second is that different mitotic stages, such as the prophase, metaphase and anaphase–telophase, are available. Third, the use of colchicine, a powerful antimitotic substance which can induce additional chromosomal alterations, can be avoided.

## MATERIALS AND METHODS

### Chemicals

The complexes were prepared according to the previously reported neutralization method,[14] i.e. by refluxing methanolic suspensions of the free L-homocysteic acid and of triorganotin(IV) hydroxides. The soluble complexes were subsequently recovered by cooling in a refrigerator and filtering through a Millipore filter, dried

 

**Table 1.** Analytical data (calculated percentages in parentheses) and Mössbauer parameters of $R_3Sn$(L-HCA) derivatives (R = Me, $^n$Bu, Ph) at liquid-nitrogen temperature

| Compound[a] | M.p. (°C) | Analysis (%) C | H | N | S | Sn | $\delta$[b] (mm s$^{-1}$) | $\lvert\Delta E\rvert_{exp}$[c] (mm s$^{-1}$) | $\Delta E_{calcd}$[d] (mm s$^{-1}$) |
|---|---|---|---|---|---|---|---|---|---|
| $Me_3Sn$(L-HCA) | 242 (dec.) | 24.10 (24.37) | 5.16 (4.68) | 3.82 (4.06) | 9.25 (9.29) | 33.24 (34.41) | 1.43 | 3.91 | −3.69 |
| $^nBu_3Sn$(L-HCA) | 80 | 40.51 (40.69) | 7.44 (7.47) | 3.01 (2.96) | 6.97 (6.79) | 23.14 (25.13) | 1.45 | 3.66 | −3.69 |
| $Ph_3Sn$(L-HCA) | 262 (dec.) | 48.13 (49.75) | 4.41 (4.17) | 2.17 (2.64) | 5.99 (6.04) | 21.53 (22.35) | 1.31 | 3.18 | −3.24 |

[a] L-HCA, L-homocysteate; sample thickness ranged between 0.50 and 0.60 mg $^{119}$Sn cm$^{-2}$.
[b] Isomer shift, $\delta \pm 0.03$ mm s$^{-1}$ with respect to $BaSnO_3$.
[c] Nuclear quadrupole splitting, $\lvert\Delta E\rvert_{exp} \pm 0.02$ mm s$^{-1}$.
[d] Regular tbp structures of tin (Fig. 19) were assumed to estimate the nuclear quadrupole splittings according to the point-charge model for $R_3Sn$(L-HCA) derivatives.

under vacuum and analyzed for C, H, N and S content at the Laboratorio di Chimica Organica (Università di Padova). Tin content was determined in our laboratory according to standard methods[15] (Table 1). L-Homocysteic acid was an ICN Biochemicals (Cleveland, Ohio) product and was used without any further recrystallization. Triorganotin(IV) hydroxides were freshly prepared by hydrolysis of triorganotin(IV) chloride parents[16,17] (gifts from Witco GmbH, Bergkamen).

IR spectra were recorded, as Nujol and hexachlorobutadiene mulls, on a Perkin-Elmer grating spectrometer Model 983G, between CsI windows.

The spectra were analyzed using a Perkin-Elmer 3600 data station with Perkin-Elmer PE983 software (Table 2).

The $^{119}$Sn Mössbauer spectra (Table 1), were measured with a multichannel analyzer (TAKES Model 639, Ponteranica, Bergamo, Italy) and a Wissenschaftliche Elektronik system (MWE, München, Germany) consisting of an MR250 driving unit, an FG2 digital function generator and an MA250 velocity transducer, moved at linear velocity, constant acceleration, in a triangular waveform. The spectra were obtained at liquid-nitrogen temperature using a DN700 liquid-nitrogen cryostat with a DN1726 sample holder and a model ITC 502 temperature controller manufactured by Oxford Instruments (Oxford, UK). The temperature control was better than ±0.1 K. The multichannel calibration was performed with an enriched iron foil

**Table 2.** Assignment of more relevant IR bands for L-homocysteic acid, L-HCAH, and the corresponding triorganotin(IV) complexes, $R_3Sn$(L-HCA) (R = Me, $^n$Bu, Ph) in the 4000–250 cm$^{-1}$ region[a, b]

| L-HCAH | $Me_3Sn$(L-HCA) | $^nBu_3Sn$(L-HCA) | $Ph_3Sn$(L-HCA) | Assignment |
|---|---|---|---|---|
| 2720–2500bd | 2720–2500bd | 2720–2500bd | 2720–2500bd | $\nu$(NH) in $NH_3^+$ |
| 1736s | | | | $\nu$(C=O) in COOH |
| | 1630s | 1639s | 1630s | $\nu_{as}(COO^-)$ |
| | 1490m | 1510s | 1513s | $\nu_s(COO^-)$ |
| 1325w | 1340w | 1338w | 1335w | |
| 1160s | 1170s | 1168s | 1151s | $\nu$ (SO) in $SO_3^-$ |
| | 550w | | | $\nu_{as}(SnC_2)$ |
| | 530w | | | $\nu_s(SnC_2)$ |
| | | | 450s | Sn-Ph |
| | 140 | 129 | 117 | $\Delta\nu$ (cm$^{-1}$) |

[a] L-HCA, L-homocysteate; Nujol and hexachlorobutadiene mulls; s, strong; w, weak; bd, broad.
[b] $\Delta\nu = [\nu_{as}(COO^-) - \nu_s(COO^-)]$.

 

**Table 3.** Experimental Mössbauer parameter, isomer shift $\delta$ mm s$^{-1}$, and calculated partial charge on tin atoms, $Q_{Sn}$(CHELEQ)[33–35], for $R_3Sn$(L-HCA) compounds and for homologous series of pentacoordinated triorganotin(IV) complexes

| Compound[a] | $\delta$[b] (mm s$^{-1}$) | $Q_{Sn}$[b] | Point no.[c] |
|---|---|---|---|
| $Alk_3SnCl$ | 1.51 | 0.097 | 1 |
| $Alk_3SnCN$ | 1.36 | 0.134 | 2 |
| $Alk_3SnNCO$ | 1.43 | 0.160 | 3 |
| $Ph_3SnCl$ | 1.35 | 0.167 | 4 |
| $Ph_3SnNCS$ | 1.40 | 0.198 | 5 |
| $Ph_3SnNCO$ | 1.20 | 0.229 | 6 |
| $Ph_3SnF$ | 1.22 | 0.252 | 7 |
| $Alk_3SnClpenGNa$ | 1.40 | 0.128 | 8 |
| $Ph_3SnClpenGNa$ | 1.30 | 0.208 | 9 |
| $Alk_3Sn$(L-HCA) | 1.44 | 0.186 | 10 |
| $Ph_3Sn$(L-HCA) | 1.31 | 0.256 | 11 |

[a] L-HCA, L-homocysteate; penG, penicillinG.
[b] Average of the isomer shifts $\delta$, and of partial atomic charge on tin atom, $Q_{Sn}$(CHELEQ), calculated or reported in Ref. 6.
[c] Identification numbers of the points in Fig. 20.

($^{57}$Fe = 99.99%, thickness 0.06 mm, DuPont, MA, USA), at room temperature, by using a $^{57}$Co–Pd source (10 mCi, DuPont, MA, USA), while the zero point of the Doppler velocity scale has been determined, at room temperature, through absorption spectra of natural $CaSnO_3$ ($^{119}$Sn = 0.5 mg cm$^{-2}$), using a $Ba^{119}SnO_3$ source (10 mCi; Amersham, UK).

The $^1$H and $^{13}$C NMR spectra in DMSO-$d_6$ solution were recorded with either an AC 250E or an AM400 Bruker spectrometer, operating at 5.87 and 9.40 T, respectively, using tetramethylsilane (TMS) as an internal standard. The relevant NMR parameters are shown in Tables 4 and 5.

Hexadeuterodimethyl sulfoxide (MDSO-$d_6$) was a Merck (Darmstadt, Germany) UVASOL reagent (>99.9% deuteration).

## Biological methods

*Paracentrotus lividus* specimens employed in the present investigation were collected from the Gulf of Palermo, in advance of the spawning period of the main population. Specimens, identified according to the guidelines of Tortonese,[18] were reared in aerated aquarium. A supply of gametes for experimental purposes was extracted directly from male and female specimens. Fertilizations were carried out using a gamete concentration of about 150–200 eggs ml$^{-1}$ and 1500–2000 sperms egg$^{-1}$. Freshly collected and filtered seawater was used throughout this investigation.

Two to four cell embryos (Figs 1 a, b) were incubated in the presence of light in separate solutions, at different concentrations and exposure times, with free L-homocysteic acid, the triorganotin(IV)L-homocysteate derivatives, triorganotin(IV) chlorides (positive controls) and in simple seawater (negative controls). Chromosome preparations were obtained from treated and untreated embryos, always in the absence of colchicine, according to the squash method, as previously described.[7]

Embryos were washed in freshly prepared 50% acetic acid fixative for 5 min, then stained in 50% acetic orcein for about 15 min, washed in

**Table 4.** $^1$H NMR parameters (chemical shifts and coupling constants) of $R_3Sn$(L-HCA) (R = Me, $^n$Bu, Ph; L-HCA, homocysteate) complexes at 298 K ($B_0$ = 5.87 or 9.40 T)

| Compound | $\delta$ (ppm)[b] $\alpha$-CH | $\beta$-$CH_2$ | $\gamma$-$CH_2$ | $NH_3^+$ | $\alpha'$-$CH_2$ or $CH_3$ | $\beta'$-$CH_2$ | $\gamma'$-$CH_2$ | $\delta$-$CH_3$ |
|---|---|---|---|---|---|---|---|---|
| L-HCAH[a] | 4.13[c] | 2.21; 2.14[d] | 2.69[c] | 8.34 | | | | |
| $Me_3Sn$(L-HCA) | 3.67[c] | 2.14; 2.00[d] | 2.63[c] | 7.90 | 0.50 $^2J_{(Sn-H)}$ = 69.7 Hz | | | |
| $^nBu_3Sn$(L-HCA) | 3.82[c] | 2.20; 2.04[d] | 2.67[c] | 8.05 | 1.14 $^2J_{(Sn-H)}$ = 62.8 Hz | 1.63[c] | 1.34[c] | 0.92[c] |
| | | | | | *ortho* | | *meta + para* | |
| $Ph_3SnL$ | 3.80[c] | 2.18; 2.02[d] | 2.59[c] | 8.02 | 7.86[c] $^3J_{(Sn-H)}$ = 64.3 Hz | | 7.49[c] | |

[a] L-HCAH, L-homocysteic acid.
[b] From TMS.
[c] Center of multiplet.
[d] Non-equivalent protons, centers of multiplets.

 

**Table 5.** $^{13}C$ NMR parameters (chemical shifts and coupling constants) of the $R_3Sn(IV)$(L-HCA) (R = Me, $^n$Bu, Ph; L-HCA, homocysteate) complexes at 298 K ($B_0$ = 5.87 or 9.40 T)

| Assignment | $\delta$ (ppm)[a] L-HCAH[b] | $Me_3Sn$(L-HCA) | $^nBu_3Sn$(L-HCA) | $Ph_3Sn$(L-HCA) |
|---|---|---|---|---|
| COOH | 170.96 | 172.02 | 171.86 | 171.81 |
| $\alpha$-C | 51.82 | 52.95 | 52.96 | 52.92 |
| $\beta$-C | 26.31 | 26.91 | 26.81 | 26.81 |
| $\gamma$-C | 47.46 | 47.99 | 48.03 | 47.71 |
| C-1 or $\alpha'$-C | | 0.61 | 18.95 | 142.72 |
| | | $^1J_{(^{119}Sn-^{13}C)}$ = 532.5 Hz | $^1J_{(^{119}Sn-^{13}C)}$ = 483.4 Hz | |
| | | $^1J_{(^{117}Sn-^{13}C)}$ = 511.3 Hz | $^1J_{(^{117}Sn-^{13}C)}$ = 462.1 Hz | |
| C-2,6 or $\beta'$-C | | | 27.78 | 136.34 |
| | | | $^2J_{(Sn-C)}$ = 27.5 Hz | $^2J_{(Sn-C)}$ = 45.2 Hz |
| C-3,5 or $\gamma'$-C | | | 26.65 | 128.58 |
| | | | $^3J_{(Sn-C)}$ = 77.0 Hz | $^3J_{(Sn-C)}$ = 70.1 Hz |
| C-4 or $\delta'$-C | | | 13.81 | 129.21 |

[a] From TMS
[b] L-HCAH, L-homocysteic acid.

50% acetic acid to remove excess of orcein, and finally each embryo was gently squeezed between a slide and its cover. Mitotic chromosomes were classified according to the Levan *et al*. terminology.[19] Chromosome preparations were examined using a Jenamed 2 phase-contrast microscope and mitotic stages were photographed with an Agfa Gevaert AG 25 film.

## RESULTS AND DISCUSSION

### Negative controls

After two hours from the beginning of experiments, embryos were always at the 16–32 blastomere stage (Fig. 2). Chromosomal observations were made on five embryos per experiment.

At the metaphase stage, each spread had 36 chromosomes which were homogeneously stained, and well separated from one another (Fig. 3). In about 60% of analyzed spreads, an evident stretch involved the centromeric region of each chromosome which was mainly located in a terminal or subterminal position (Fig. 4).

At the anaphase stage, chromosomes formed two distinct groups, each containing 36 elements directed towards the opposite polar regions of the mitotic spindle (Fig. 5; one group is represented). Association of elements of one group with elements of the other was occasionally encountered (2–3%). Additional chromosomal alterations were not detected. After six hours embryos could be observed at the blastula stage (Fig. 6). Equal numbers of prophases, metaphases and anaphase–telophases occurred in this stage after karyological analysis. Structural chromosomal alterations such as breakages and

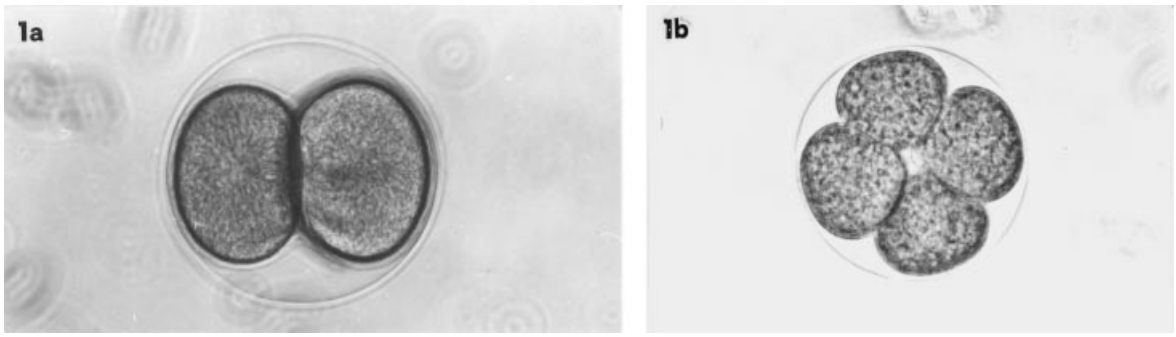


**Figure 1** Early-developing embryos: (a) at two-blastomere stage; (b) at four-blastomere stage.

 

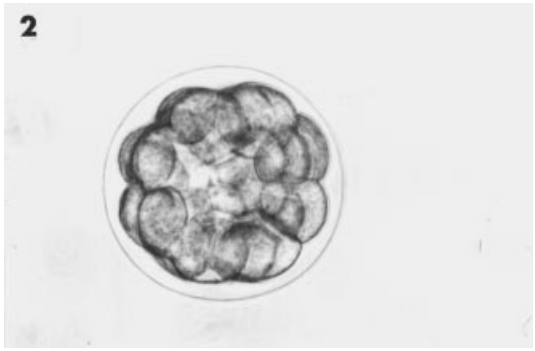


**Figure 2** Embryo at 16–32 blastomere stage.

overcondensed areas were rarely observed (1–2%).

After 18 h embryos were at the gastrula stage (Fig. 7) so that each of them consisted of a high number of cells. Analyzed spreads of embryos, at this stage, showed chromosomes close to one another. Consequently, they were not individually detectable. Despite this, identification of the mitotic stage of each spread was possible, thus allowing us to establish that nearly identical numbers of prophases, metaphases and anaphase–telophases occurred (Fig. 8). Moreover, it could be observed that about 50% of metaphases

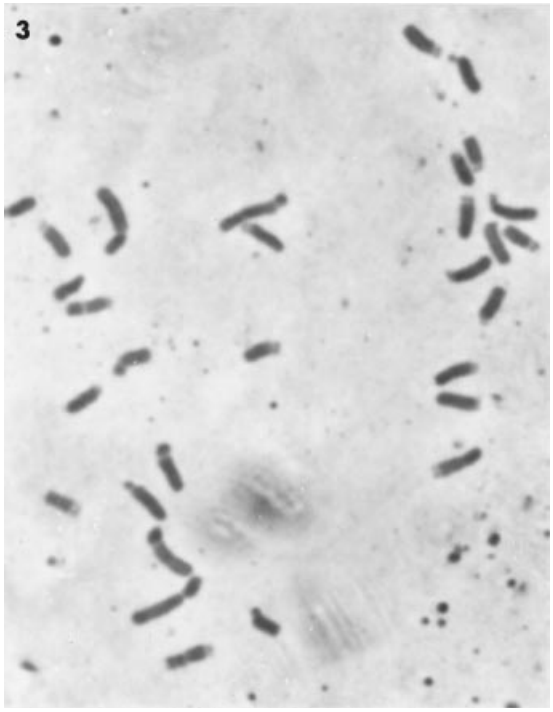


**Figure 3** Metaphase chromosomes in controls.

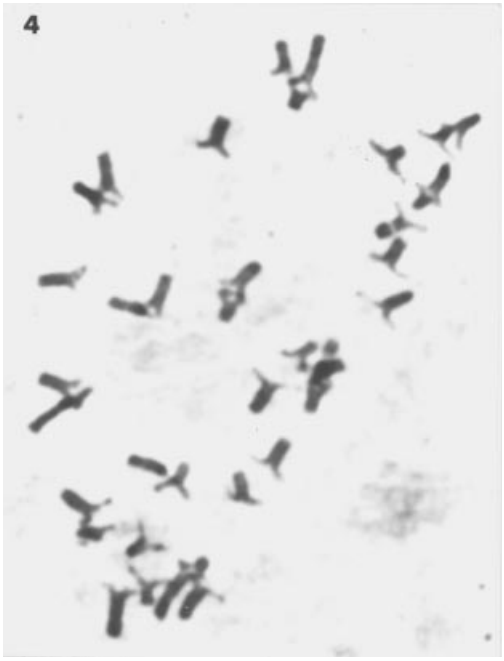


**Figure 4** Metaphase chromosomes with centromeric stretch in controls.

were characterized by the presence of a stretch among sister chromatids, involving the centromeric region of each chromosome, and only about 1% of anaphases showed bridges between chromosomes of the two groups.

## Embryos treated with free L-homocysteic acid or triorganotin(IV) L-homocysteate derivatives

Experimental conditions and results obtained after analyses of metaphase and anaphase chromosomes of five embryos per experiment are summarized in Table 6.

Chromosomal anomalies mainly occurred following exposure to $R_3Sn$(L-HCA) (R = Me, $^n$Bu) at $10^{-7}$ mol $l^{-1}$. Instead, treatment of embryos with $R_3Sn$(L-HCA) (R = Me, $^n$Bu, Ph) at $10^{-5}$ mol $l^{-1}$ and $Ph_3Sn$(L-HCA) at $10^{-7}$ mol $l^{-1}$ resulted in arrest of development. In fact, a high percentage of embryos proportional to exposure time, displayed blastomeres with anomalous surfaces due to the occurrence of extrusions (Fig. 9). Also, alteration of spatial disposition of blastomeres forming each embryo was observed (Fig. 10 a, b). Aberrant chromosomes at the metaphase stage mainly appeared as deeply

 

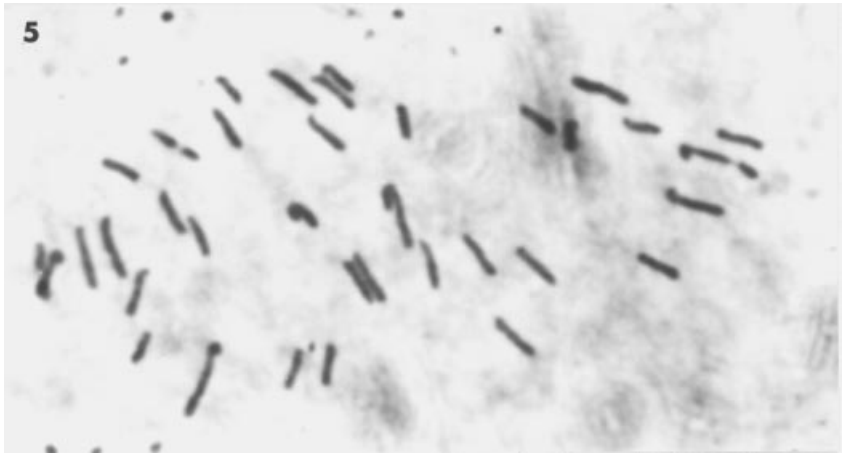


**Figure 5** Diploid set of anaphase chromosomes in controls.

stained bodies invariably without stretch among sister chromatids (Fig. 11), or appearing as roundish-shaped bodies which were often closely associated in groups (Fig. 12). The results of structural chromosome damage could be observed in anaphase cells as bridges between the separating chromosomes involving one (Figs 13 a, b), or more than one, chromosome pair per spread (Fig. 14). Chromosomes (one or more per spread) also appeared with breakages looking


**Figure 6** Embryo at blastula stage after 6 h in controls.


**Figure 7** Embryo at gastrula stage after 18 h in controls.

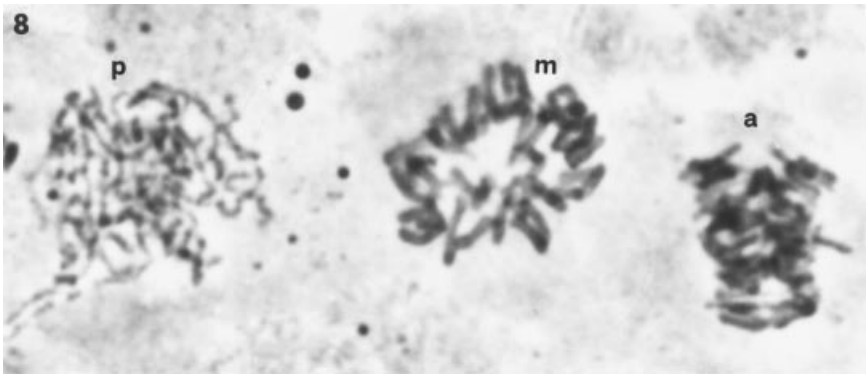


**Figure 8** Different mitotic stages in control embryos after 18 h: p, prophase; m, metaphase; a, anaphase.

 

like chromatic lesions or 'gaps' (Fig. 15), or with small, deeply stained granular areas, mainly located at the telomeric chromosomal region (Fig. 16). Results quite similar to those induced by the action of the triorganotin(IV) L-homocysteate derivatives were obtained following exposure of two to four blastomere embryos to the organotin(IV) chlorides, while, as in negative controls, chromosomal aberrations were occasionally encountered in embryos incubated in free L-homocysteic acid solutions.

$R_3Sn$(L-HCA) (R = Me, $^n$Bu, Ph) were tested also at a $10^{-9}$ mol $l^{-1}$ concentration as well. At this concentration chemicals employed in this study did not produce significant chromosomal alterations or anomalies in the embryo development.

Development seemed to parallel that of the control for the whole time of the experiment (18 h) after incubation of two to four cell embryos either in $Me_3Sn$(L-HCA) or in its parent at $10^{-7}$ mol $l^{-1}$ solution. Analysis of chromosomal preparations of these embryos, instead, showed that the rate 1:1:1 consistently observed among prophase, metaphase and anaphase–telophase in the negative controls, varied in treated embryos. The experimental results illustrated in the histograms of Fig. 17 clearly show that both prophases and anaphase–telophases decreased and that such a decrease was closely related to the length of exposure.

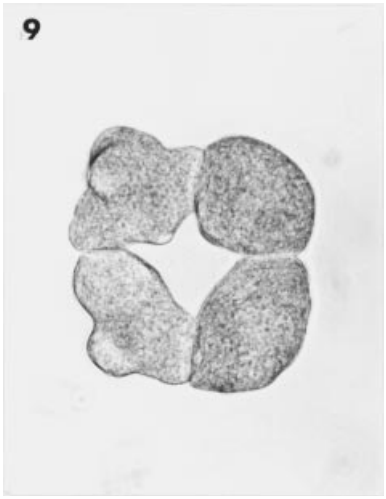


**Figure 9** Anomalous embryos arrested at four-blastomere stage treated with $10^{-5}$ mol $l^{-1}$ $^n Bu_3Sn$(L-HCA) solution after 2 h.

## The chemical investigation

The solid-state investigation of the complexes obtained was carried out by IR and Mössbauer spectroscopy. The comparison of the IR spectra of the agonist L-homocysteic acid, free and coordinated to the triorganotin(IV) moieties, is noteworthy in order to identify the donor atoms coordinating the tin atoms. The experimental Mössbauer parameters–isomer shift, $\delta$ (mm $s^{-1}$), and quadrupole splittings, $\Delta E$(mm $s^{-1}$)—provide charge-density and molecular geometry data around the tin atoms.

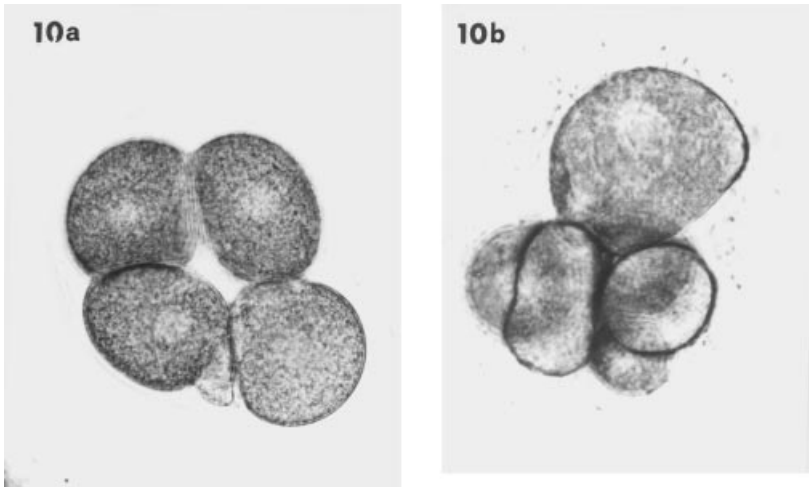


**Figure 10** Damaged embryos arrested at four-blastomere stage: (a) treated with $10^{-5}$ mol $l^{-1}$ $Me_3Sn$(L-HCA) solution, (b) treated with $10^{-5}$ mol $l^{-1}$ $Ph_3Sn$(L-HCA) solution.

 

**Infrared spectra of triorganotin(IV) (L-HCA) derivatives [$R_3Sn$(L-HCA); R = Me, $^n$Bu, Ph]**

L-Homocysteic acid is a potential polydentate bianionic ligand when exerting its coordinating power towards the Lewis acids. In fact, the carboxylate oxygen atoms, the amino nitrogen and the oxygen atoms of the sulfonate group may act as donor atoms. The more relevant IR absorptions of the free L-homocysteic acid are summarized in Table 2, together with those of its triorganotin(IV) derivatives, for comparison.[20–23]

In particular, in the range 2720–2500 $cm^{-1}$, the free L-homocysteic acid shows: (1) a series of broad bands attributable to the $\nu$(NH) stretching of $NH_3^+$ group; (2) an absorption due to $\nu_{as}$(COOH), at 1736s $cm^{-1}$, and (3) bands characteristic of $\nu$(SO) in —$SO_3^-$, at 1325w and 1160s $cm^{-1}$.[24] Altogether these findings suggest the structure of the L-homocysteic acid represented in Fig. 18.

The triorganotin(IV) L-homocysteate IR spectra show, in the range 2720–2500 $cm^{-1}$, the group of bands attributed in the free ligand to $\nu$(NH) of $NH_3^+$, which, together with the invariance of the $\nu$(SO) of –$SO_3^-$, would suggest the non-involvement of both the amino nitrogen and the sulfonate oxygen atoms in the coordination of the triorganotin(IV) moieties (Table 2). Bands attributable to asymmetric and symmetric stretchings of the carboxylate group at 1630s and 1490s $cm^{-1}$ in $Me_3Sn$(L-HCA) ($\Delta\nu = 140\ cm^{-1}$), at 1639s and 1510s $cm^{-1}$ in $^n Bu_3Sn$(L-HCA) ($\Delta\nu = 129\ cm^{-1}$) and at 1630s and 1513s $cm^{-1}$ in $Ph_3Sn$(L-HCA) ($\Delta\nu = 117\ cm^{-1}$), are also pre-

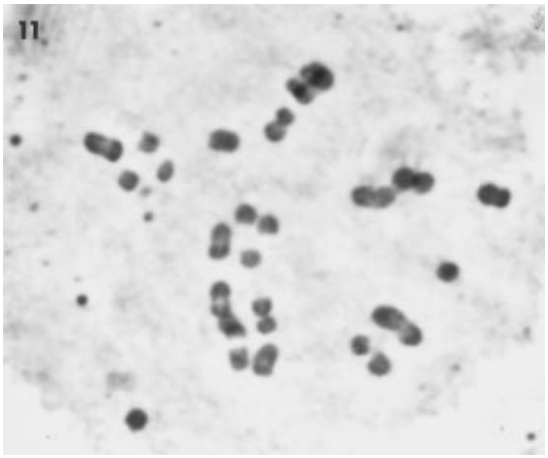


**Figure 11** Anomalous metaphase chromosomes in embryos treated with $10^{-7}$ mol $l^{-1}$ $Me_3Sn$(L-HCA) solution after 18 h (colchicinized-like chromosomes).

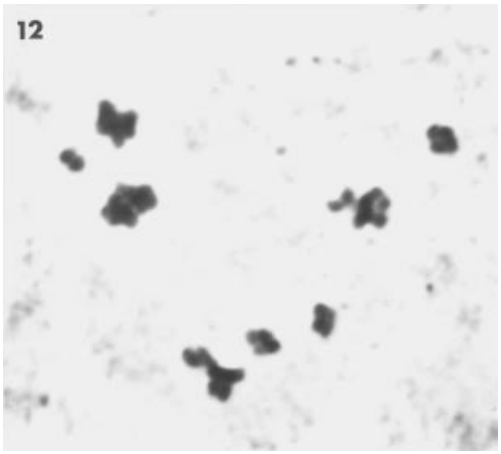


**Figure 12** Anomalous metaphase chromosomes in embryos treated with $10^{-7}$ mol $l^{-1}$ $^n Bu_3Sn$(L-HCA) solution after 2 h (see chromosomes associated in groups).

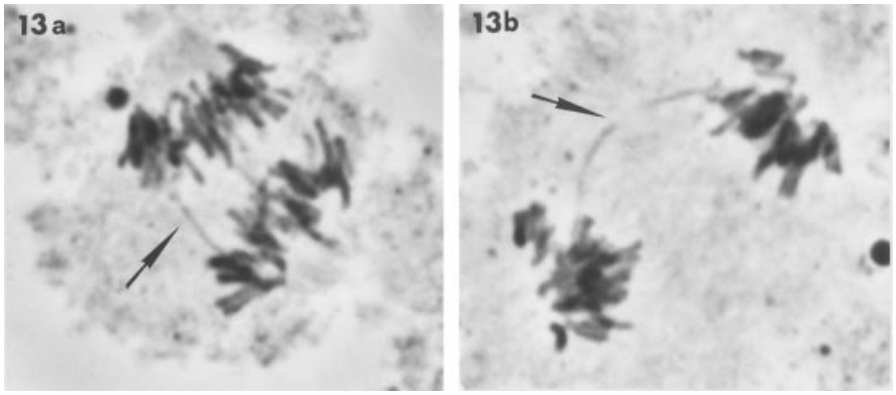


**Figure 13** Anomalous anaphase chromosomes in embryos treated with $10^{-7}$ mol $l^{-1}$ $^n Bu_3Sn$(L-HCA) solution after 6 h: (a) and (b) with a single chromosomal bridge (see arrows).

 

sent. Such values of $\Delta\nu$ are representative of chelating or bridging carboxylate groups.[22,23]

In $Me_3Sn$(L-HCA) there are two bands at 550w and 530w $cm^{-1}$ characteristic of $\nu_{as}(SnC_2)$ and $\nu_s(SnC_2)$, while at 450 $cm^{-1}$, in $Ph_3Sn$(L-HCA), the Y mode in the Wiffen notation, due to the SnPh bond, is present.[25]

The analytical data and the IR spectra of triorganotin(IV)(L-HCA) complexes suggest that the tin atom in such derivatives is at least five-coordinated, with the ligand acting as a monoanionic bidentate ligand, through a bridging or chelating carboxylate anion.

**Mössbauer spectra**

The experimental Mössbauer parameters, isomer shift $\delta$ (mm $s^{-1}$) and nuclear quadrupole splitting $|\Delta E_{exp}|$ (mm $s^{-1}$), of all the complexes are reported in Table 1, together with $\Delta E$ calculated according to the point-charge model formalism, applied to the idealized structures of Fig. 19 for $R_3Sn$(L-HCA) derivatives.[26–29]

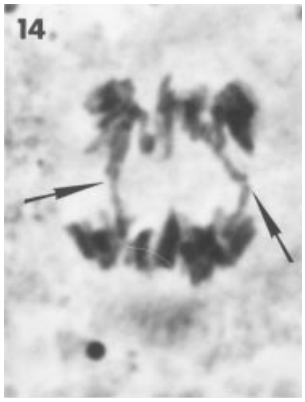


**Figure 14** Anomalous anaphase chromosomes in embryos treated with $10^{-7}$ mol $l^{-1}$ $Me_3Sn$(L-HCA) solution after 18 h (arrows indicate chromosomal bridges).

The isomer shift $\delta$, a consequence of the electrostatic interaction between the nuclear charge distribution and those electrons which possess a finite probability to be in the nuclear region, may be calculated according to Eqn [1]:

$$\delta = K\frac{\Delta R}{R}([\psi(O)_s]^2_a - [\psi(O)_s]^2_s) \qquad [1]$$

where $[\psi(O)_s]^2_a$ and $[\psi(O)_s]^2_s$ are the total 5*s* electronic density at the nucleus of respectively, the absorber and the source tin atoms, $K$ is a constant characteristic for the $^{119}$Sn atom, and $\Delta R$ is equal to $(R_{ex} - R_{ground})$ (the radii of excited and ground nuclear states, respectively) and is positive for the tin atom.[30] The $\delta$ values are, therefore, diagnostic of the nature of the bond between the Mössbauer and the ligand atoms. Comparison of the experimental $\delta$ values (Table 1) and in particular the small difference encountered in these $R_3Sn$(L-HCA) derivatives shows that the covalent character of the bonds does not vary appreciably on going from the trialkyltin(IV) to the triphenyltin(IV)(L-HCA) complexes.

Preliminary structural information on the triorganotin(IV)(L-HCA) derivatives may be obtained by correlating the isomer shift, $\delta$ mm $s^{-1}$, of the derivatives under investigation and those of congener and isostructural triorganotin(IV) halides, pseudohalides and triorganotin(IV)chloropenGNa, whose trigonal-

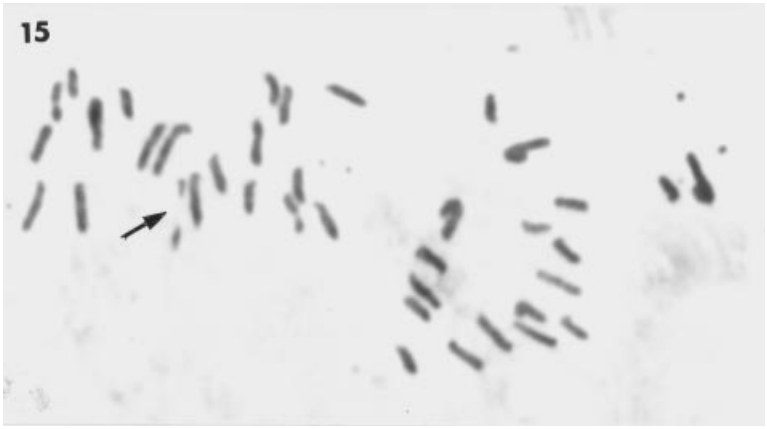


**Figure 15** Anaphase chromosomes displaying breakage (see arrow) in embryos treated with $10^{-7}$ mol $l^{-1}$ $Me_3Sn$(L-HCA) solution after 6 h.

 

bipyramidal configuration has been previously advanced,[31,32] with the partial atomic charges on tin atoms, $Q_{Sn}$, calculated according to orbital electronegativity equalization procedures (Table 3) described in the literature.[33–35] The experimental isomer shifts $\delta$ for all the derivatives of Table 3 have been subsequently plotted as a function of the partial atomic charges on tin, $Q_{Sn}$ (Fig. 20).

The dependence of $\delta$ on $Q_{Sn}$ is linear, in agreement with results obtained for a number of homologous organotin(IV) compounds.[31,32]

Finally both fingerprint criteria based on the nuclear quadrupole splittings, $\Delta E$ mm s$^{-1}$, and their rationalization according to the point-charge model formalism[26–29] applied to the idealized trigonal-bipyramidal structure of Fig. 19, confirm for $R_3Sn$(L-HCA) derivatives the geometry proposed on the basis of the previously discussed relation between $\delta$ and $Q_{Sn}$.

It must be pointed out that there is a good agreement between experimental and calculated $\Delta E$ (Table 1), to less than $\pm 0.4$ mm s$^{-1}$ maximum difference allowed between experimental and calculated $\Delta E$, which allows us to accept the assumed geometry of Fig. 19.[29]

**NMR spectra**

The $^1$H NMR parameters of the organotin(IV) derivatives of L-homocysteic acid, L-HCAH, are shown in Table 4. The integrated intensities of the spectra clearly indicate a 1:1 metal-to-ligand stoichiometry in solution, in agreement with the analytical data on the solids.

Tin satellites are observed, from which the coupling constants to tin can be obtained, though the $^{119}$Sn and $^{117}$Sn couplings are generally not resolved.

From the two-bond couplings, $^2J$, the C–Sn–C angle, $\theta$, can be evaluated by means of the Lockhart equation[36] (Eqn [2]).

$$\theta = 0.0161|^2J(^{119}\text{Sn}, ^1\text{H})|^2 - 1.32|^2J(^{119}\text{Sn}, ^1\text{H})| + 133.4 \qquad [2]$$

The $\theta$ values derived for the trimethyltin(IV) and tributyltin(IV) complexes are 120° and 114°, respectively. This result suggests pentacoordination of tin, with the alkyl groups in the equatorial

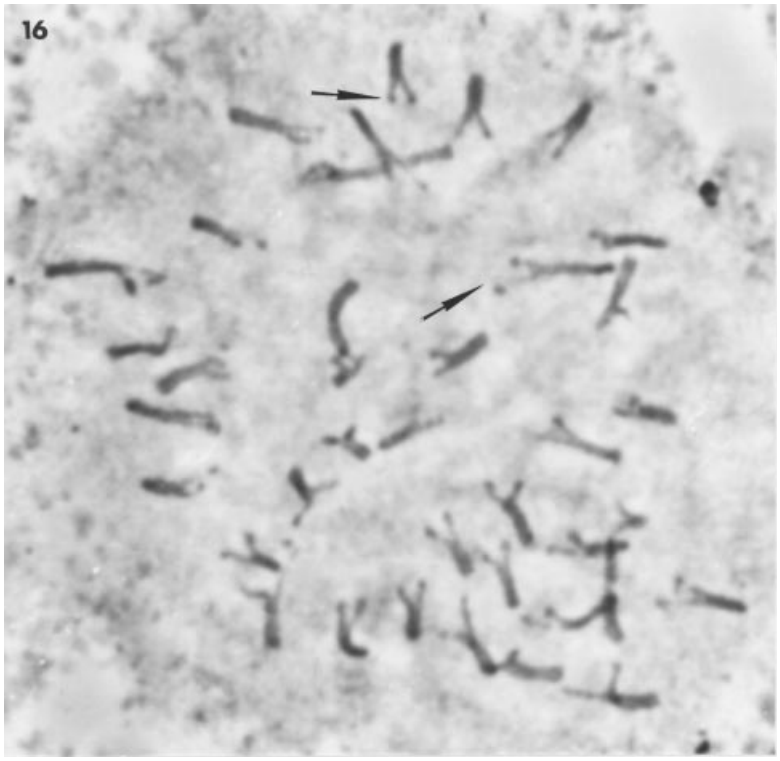


**Figure 16** Metaphase chromosomes displaying overcondensed telomeric regions (see arrow) in embryos treated with $10^{-7}$ mol l$^{-1}$ $^n$Bu$_3$Sn(L-HCA) solution after 6 h.

 

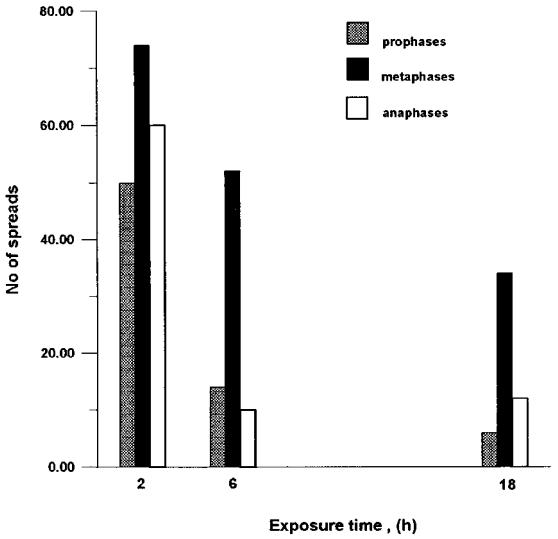


**Figure 17** Histograms displaying amounts of mitotic stages at different exposure times in embryos treated with $10^{-7}$ mol $l^{-1}$ $Me_3Sn$(L-HCA).

plane of a more or less distorted trigonal bipyramid, in agreement with the conclusions drawn from IR and Mössbauer data. The $NH_3^+$ group does not seem to be involved in the coordination scheme, converting to $NH_2$, since the area of the peak always corresponds to nearly three protons. This finding is in agreement with IR and Mössbauer conclusions for the complexes in the solid state. The $^{13}C$ NMR parameters are shown in Table 5. Only for $Me_3Sn^{IV}$ and $^nBu_3Sn^{IV}$ complexes was the solubility high enough to allow detection of the tin satellites and thus the determination of $^1J(^{119}Sn, ^{13}C)$. From these couplings (Table 5) the angle $\theta$ can be evaluated by means of Eqn [3],[36] and the values of 119° and 123° were derived for the tributyltin(IV) and the trimethyltin(IV) L-homocysteate, respectively, again in agreement with the other experimental results, which suggest a trigonal bipyramid as the coordination polyhedron with equatorial organic groups (Fig. 19).

$$^1J = 11.4\theta - 875 \qquad [3]$$

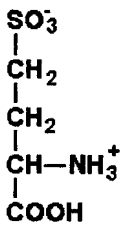


**Figure 18** L-Homocysteic acid (L-HCAH).

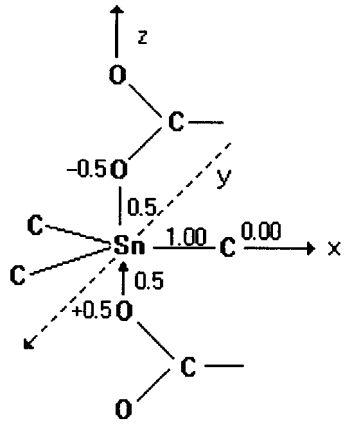


**Figure 19** Regular trigonal-bipyramidal (tbp) structures of tin assumed to estimate both the nuclear quadrupole splittings according to the point-charge model (Table 1) and the partial atomic charge on the tin atom, $Q_{Sn}$, (see text and Table 3), $R_3Sn$(L-HCA) derivatives. *x*, *y* and *z* are the directions of the principal components of the electric field gradient (e.f.g.) ($|V_{zz}| >> |V_{yy}| >> |V_{xx}|$); off-diagonal components of e.f.g. are diagonalized. The partial quadrupole splittings (p.q.s.; mm $s^{-1}$) used in the calculations are: $\{Ph\}^{tbe} = -0.98$; $\{COO^-\}^{tba}_{bridg} = 0.075$ (see Refs 26–29). The reported bond orders and formal charges are assumed as input in the calculation of the partial atomic charge on the tin atom, $Q_{Sn}$.

Long-range couplings to tin are also observed in a few cases (see Table 5) and the common trend $^3J > ^2J$ is observed.[37]

## The biological investigation

As previously reported for organotin(IV)chloro derivatives of penicillin G and organotin(IV) amoxicillin derivatives,[7,9] for organotin(IV) L-homocysteate derivatives also data summarized in Table 6 suggest three implications.

1. Triorganotin(IV) L-homocysteate derivatives and their triorganotin(IV) chloride parents used in this study as positive control materials, due to their established activities,[38] are both toxic. In contrast, free L-homocysteic acid exerts no significant toxic activity towards developing *P. lividus* embryos. This would primarily suggest that toxicity of the triorganotin(IV) L-homocysteates is due to the action of the organometallic moieties contained in these chemicals.

2. Trimethyltin(IV) L-homocysteates are less toxic than the corresponding butyl and phenyl derivatives, the assumption being based on the fact that development is arrested when embryos

 

are treated with triorganotin(IV) L-homocysteates containing the latter organic groups at concentrations of $10^{-7}$ mol $l^{-1}$. $R_3SnL$ solutions, at $10^{-9}$ mol $l^{-1}$ concentration, did not produce any significant chromosomal alteration after 18 hours. However genotoxicity of $R_3SnL$ compounds at $10^{-7}$ mol $l^{-1}$ seems to parallel the length of exposure. Consequently, this might imply that a concentration of $10^{-9}$ mol $l^{-1}$ of these chemicals could result in chromosomal damage after exposure times longer than 18–20 h. Unfortunately, technical reasons prevented chromosomal analyses of these embryos due to their very advanced stage of development.

In comparison with controls (Table 6), a substantial increase in structural chromosomal aberrations could be observed in embryos where development was not arrested. Anomalies are related to the length of exposure time and include

(a) unstained portions, explained as chromosomal regions of much reduced DNA content (gaps) (these might have originated following errors in packing during chromosome condensation);[39]

(b) overcondensed areas resulting in small deeply stained regions which, in the common sea urchin *P. lividus*, appeared to be consistently located at the chromosomal telomeric regions;

(c) alterations involving the mitotic process because chromosomes resulted that were deprived of the centromeric stretch among sister chromatids;

(d) chromosomes often closely connected in groups.

Such modifications, involving mitotic chromosomes, most closely resemble the effects of colchicine treatment already reported for the chromosomes of the atlantic mackerel *Scomber scombrus* following exposure to contaminants containing heavy metals,[40] and for chromosomes of human lymphocytes following exposure to inorganic and organic lead compounds.[41] Similar results were obtained also in spermatogonial chromosomes of *Truncatella subcylindrica* (Mollusca, Mesogastropoda) treated with dibutyltin(IV)dichloride and tributyltin(IV)

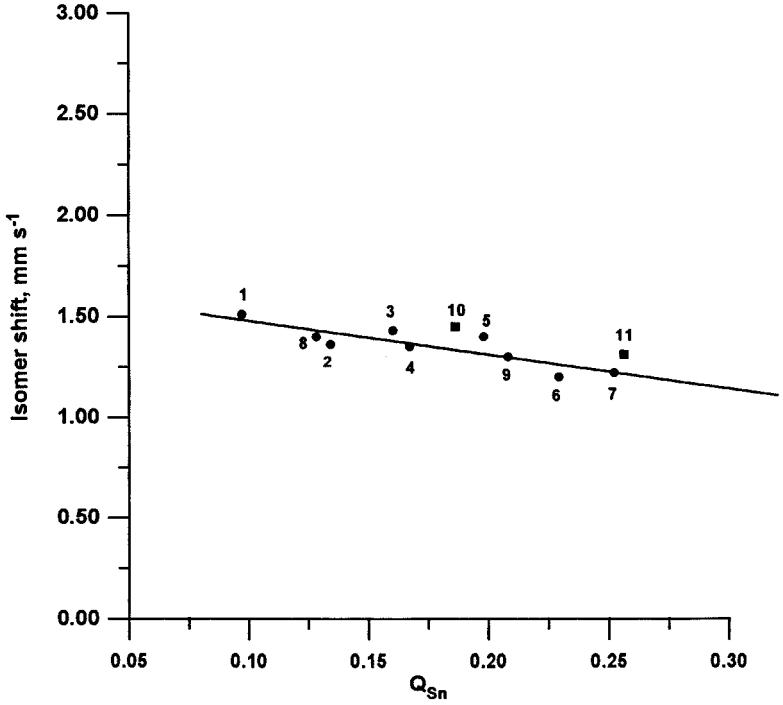


**Figure 20** Isomer shifts $\delta$ versus atomic charge, $Q_{Sn}$, for $R_3Sn$(L-HCA) derivatives (■, point nos 10 and 11, Table 3), and structurally correlated complexes (●, points 1–9, Table 3). Full line is the least-squares fit of data points 1–9 (●, Table 3).

 

chloride.[38]

3. Results of this investigation also suggest that aneuploid telophase nuclei (e.g. nuclei containing different chromosome numbers) can be formed under the action of triorganotin(IV) L-homocysteates. In fact, the presence of the chemicals in the solutions used in our experiments significantly increases the rate of chromosomal bridges appearing as thin strands of thread-like chromatin among daughter chromosomes at anaphase. Such events are explained as originating from chromosomal breakages and translocations, followed by rejoining of the broken ends in abnormal patterns, and are commonly thought to be mainly responsible for non-disjunction of separating chromosomes. All

**Table 6.** Genotoxic activity: mitotic metaphase and anaphase chromosomal damage in *Paracentrotus lividus* embryos treated with $R_3SnCl$ and $R_3Sn$(L-HCA)[a] (R = Me, $^n$Bu, Ph)

| Compound | Concentration (mol $l^{-1}$) | Time interval (h) | No. of spreads | | | | |
|---|---|---|---|---|---|---|---|
| | | | Normal | Irregular staining | Granular zones | Colchicinized-like chromosomes | Total spreads |
| Control | | 2 | 71 | 2 | 1 | 0 | 74 |
| | | 6–8 | 110 | 0 | 4 | 0 | 114 |
| | | 18–20 | 258 | 3 | 3 | 0 | 264 |
| $Me_3Sn$(L-HCA) | $10^{-5}$ | 2 | Arrest | | | | |
| | | 6–8 | | | | | |
| | | 18–20 | | | | | |
| | $10^{-7}$ | 2 | 6 | 8 | 8 | 20 | 42 |
| | | 6–8 | 4 | 6 | 3 | 25 | 38 |
| | | 18–20 | 0 | 0 | 0 | 5 | 5 |
| $Me_3SnCl$ | $10^{-5}$ | 2 | Arrest | | | | |
| | | 6–8 | | | | | |
| | | 18–20 | | | | | |
| | $10^{-7}$ | 2 | 4 | 10 | 12 | 15 | 41 |
| | | 6–8 | 4 | 4 | 5 | 20 | 33 |
| | | 18–20 | 0 | 0 | 3 | 7 | 10 |
| $^nBu_3Sn$(L-HCA) | $10^{-5}$ | 2 | Arrest | | | | |
| | | 6–8 | | | | | |
| | | 18–20 | | | | | |
| | $10^{-7}$ | 2 | 4 | 6 | 6 | 12 | 28 |
| | | 6–8 | 0 | 3 | 5 | 20 | 28 |
| | | 18–20 | Arrest | | | | |
| $^nBu_3SnCl$ | $10^{-5}$ | 2 | Arrest | | | | |
| | | 6–8 | | | | | |
| | | 18–20 | | | | | |
| | $10^{-7}$ | 2 | 7 | 12 | 6 | 15 | 40 |
| | | 6–8 | 2 | 4 | 4 | 26 | 36 |
| | | 18–20 | Arrest | | | | |
| $Ph_3Sn$(L-HCA) | $10^{-5}$ | 2 | Arrest | | | | |
| | | 6–8 | | | | | |
| | | 18–20 | | | | | |
| | $10^{-7}$ | 2 | Arrest | | | | |
| | | 6–8 | | | | | |
| | | 18–20 | | | | | |
| $Ph_3SnCl$ | $10^{-5}$ | 2 | Arrest | | | | |
| | | 6–8 | | | | | |
| | | 18–20 | | | | | |
| | $10^{-7}$ | 2 | Arrest | | | | |
| | | 6–8 | | | | | |
| | | 18–20 | | | | | |

[a] L-HCA, L-homocysteate.

 

of these effects may lead to inaccurate distribution of chromosomes between daughter nuclei, resulting in cells with chromosomal numbers that deviate from the normal diploid complement. Identical conclusions have been reached using bone-marrow micronucleus tests after treatment with the crude extract of *Macrocystis pyrifera*,[42] two continuous cell lines, rainbow trout gonad (RTG-2) and bluegill fry (BF-2) following exposure to four polycyclic aromatic hydrocarbons (PAH), aromatic amine, one nitrosamide and one fungal toxine,[43] and early developing embryos of *Anilocra physodes* (Crustacea, Isopoda) following exposure to bis[dimethyltin(IV)chloro] protoporphyrin IX.[44]

As suggested in a previous report,[45] the present data imply that the cytotoxic alterations, involving embryos at early stages of development, are also related to chromosomal disorders, mainly resulting in structural alterations of the chromosomes and/or inhibition of mitotic spindle, this latter presumably through a modification of the chemical structure of the tubulin.

*Acknowledgements* Financial support by the Ministero per l'Università e la Ricerca Scientifica e Tecnologica (MURST), University of Palermo and by the National Research Council (C.N.R., Progetto Finalizzato—Chimica Fine), Roma, for a fellowship to T.F., are gratefully acknowledged.

## REFERENCES

1. J. C. Watkins, P. Krogsgaard-Larsen and T. Honoré, *Trends Pharmacol. Sci.* **11**, 25 (1990).
2. J. C. Watkins and L. Collingridge, *The NMDA Receptor*, Oxford University Press, Oxford, 1989.
3. J. W. Holney, M. T. Price, K. S. Shalles, J. Labruyere, R. Ryeson, K. Mahan, G. Frierdich and L. Samson, *Brain Res. Bull.* **19**, 597 (1987).
4. R. G. Feldman, R. F. White and I. I. Eriator, *Arch. Neurol.* **50**, 1320 (1993).
5. Y. Arakawa and O. Wada, Biological properties of alkyltin compounds. In: *Metal Ions in Biological Systems*, Sigel, H. and Sigel, A. (eds), Marcel Dekker, New York, 1993, Vol. 29, p. 101.
6. F. Maggio, A. Pellerito, L. Pellerito, S. Grimaudo, C. Mansueto and R. Vitturi, *Appl. Organomet. Chem.* **8**, 71 (1994).
7. R. Vitturi, C. Mansueto, A. Gianguzza, F. Maggio, A. Pellerito and L. Pellerito, *Appl. Organomet. Chem.* **8**, 509 (1994).
8. L. Pellerito, F. Maggio, M. Consiglio, A. Pellerito, G. C. Stocco and S. Grimaudo, *Appl. Organomet. Chem.* **9**, 227 (1995).
9. R. Vitturi, B. Zava, M. S. Colomba, A. Pellerito, F. Maggio and L. Pellerito, *Appl. Organomet. Chem.* **9**, 561 (1995).
10. C. Mansueto, L. Pellerito, M. A. Girasolo and M. Lo Valvo, *Appl. Organomet. Chem.* **7**, 95 (1993).
11. D. Colombera and R. Vitturi, *Caryologia* **31**, 479 (1978).
12. R. Barbieri, V. Izzo, M. Cantone, G. Duro and G. Giudice, *Rend. Fis. Acc. Lincei* **9**, 369 (1992).
13. C. Lipani, R. Vitturi, G. Sconzo and G. Barbata, *Mar. Biol.* **127**, 67 (1996).
14. B. Mundus-Glowacki, F. Huber, H. Preut, G. Ruisi and R. Barbieri, *Appl. Organomet. Chem.* **6**, 83 (1992).
15. W. P. Neumann, *The Organic Chemistry of Tin*, Interscience, London, 1970.
16. A. J. Bloodworth and A. G. Davies, Organotin compounds with Sn–O bonds. Organotin alkoxides, oxides and related compounds. In: *Organotin Compounds*, Sawyer, A. K. (ed.), Marcel Dekker, New York, 1971, Vol. 1, Chapter 4, p. 153.
17. R. S. Tobias, I. Ogrin and B. A. Nevett, *Inorg. Chem.* **1**, 638 (1962).
18. E. Tortonese, *Fauna d'Italia*, Vol. VI, *Echinodermata*, Calderini, Bologna, 1965.
19. A. Levan, K. Fredga and A. A. Sandberg, *Hereditas* **52**, 201 (1964).
20. F. A. Cotton, The infrared spectra of transition metal complexes. In: *Modern Coordination Chemistry*, Lewis, J. and Wilkins, R. G. (eds), Interscience, New York, 1960.
21. K. Nakamoto, *Infrared Spectra of Inorganic and Organometallic Compounds*, John Wiley, New York, 1963.
22. G. B. Deacon and R. J. Phillips, *Coord. Chem. Rev.* **33**, 227 (1980).
23. G. B. Deacon, F. Huber and R. J. Phillips, *Inorg. Chim. Acta* **104**, 41 (1985).
24. P. A. Yeats, J. R. Sams and F. Aubke, *Inorg. Chem.* **11**, 2634 (1972) and references therein.
25. D. H. Wiffen, *J. Chem. Soc.* 1350 (1956).
26. G. M. Bancroft and R. H. Platt, *Adv. Inorg. Chem. Radiochem.* **15**, 59 (1972).
27. G. M. Bancroft, V. G. Kumar Das, T. K. Sham and M. G. Clark, *J. Chem. Soc., Dalton Trans.* 643 (1976) and references therein.
28. R. L. Collins and J. C. Travis, The electric field gradient tensor. In: *Mössbauer Effect Methodology*, Gruverman, I. J. (ed.), Plenum Press, New York, 1967, Vol. 3, p. 123.
29. A. G. Davis, A. G. Maddock and R. H. Platt, *J. Chem. Soc., Dalton Trans* 21 (1972).
30. M. G. Clark, A. G. Maddock and R. H. Platt, *J. Chem. Soc., Dalton Trans.* 281 (1972).
31. C-D. Hager, F. Huber, A. Silvestri, A. Barbieri and R. Barbieri, *Gazz. Chim. Ital.* **123**, 583 (1993) and references therein.

 

32. L. Pellerito, F. Maggio, T. Fiore and A. Pellerito, *Appl. Organomet. Chem.* **10**, 393 (1996) and references therein.
33. W. L. Jolly and W. B. Perry, *J. Am. Chem. Soc.* **95**, 5442 (1973).
34. W. L. Jolly and W. B. Perry, *Inorg. Chem.* **13**, 2686 (1974).
35. W. B. Perry and W. L. Jolly, *The Calculation of Atomic Charge in Molecules by an Electronegativity Equalization Procedure: A Description of Program CHELEQ*, US Atomic Energy Commission, Contract W-7405-ENG-48 (Nov. 1974).
36. T. P. Lockhart and W. F. Manders, *Inorg. Chem.* **25**, 892 (1986).
37. M. Bullpitt, W. Kitching, W. Adcock and D. Doddrell, *J. Organomet. Chem.* **116**, 161 (1976).
38. R. Vitturi, C. Mansueto, E. Catalano, M. A. Girasolo and L. Pellerito, *Appl. Organomet. Chem.* **6**, 525 (1992).
39. J. R. K. Savage, *Experientia* **45**, 92 (1989).
40. A. C. Longwell and J. B. Hughes, *Rapp. P.v. Rèun. Cons. Int. Explor. Mer.* **179**, 275 (1980).
41. O. Andersen and P. Grandjean, *Appl. Organomet. Chem.* **1**, 15 (1987).
42. I. B. Larripa, M. Mudry de Pergament, M. Labal de Vinuesa and A. M. S. Mayer, *Hydrobiologia* **151/152**, 491 (1987).
43. R. M. Kocan, M. L. Landolt, J. A. Bond and E. P. Benditt, *Arch. Environ. Contam. Toxicol.* **10**, 663 (1981).
44. R. Vitturi, L. Pellerito, E. Catalano and M. R. Lo Conte, *Appl. Organomet. Chem.* **7**, 295 (1993).
45. C. Mansueto, L. Pellerito and M. A. Girasolo, *Acta Embryol. Morphol. Exper. n.s.*, **10**(3), 237 (1989).

 